学术期刊可以用微信做什么，快来看看！

可全面技术输出

微信自动应答服务平台

微时代 微革命

微服务

移动互联网时代的营销革命

简单快捷 · 高效互动 · 随时随地 · 广泛传播

微信扫一扫

开启智慧“微服务”

Recent achievements on underwater optical wireless communication [Invited]

Giulio Cossu*

Scuola Superiore Sant'Anna, TeCIP Institute, 56124 Pisa, Italy
**Corresponding author: g.cossu@santannapisa.it*

Received July 29, 2019; accepted September 12, 2019; posted online October 14, 2019

The growing number of underwater activities is giving momentum to the development of new technologies, such as buoys, remotely operated vehicles, and autonomous underwater vehicles. The data collected by these vehicles need to be transmitted to a high-speed central unit. Clearly, wired solutions are not suitable, since they strongly impact the mobility. In this scenario, a promising solution is offered by underwater optical wireless communication (UOWC) technology, which can achieve both high-speed and wireless operation. Here, we provide a comprehensive survey on the challenges, the experimental realizations, and the state of the art in UOWC researches.

OCIS codes: 060.2605, 230.3670, 140.7300, 010.7340.
doi: 10.3788/COL201917.100009.

More than 70% of the Earth's surface is covered by water. Early sea explorations sink their roots thousands of years ago with the first sailing vessels and the first navigators. Since then, the study of the oceans and marine ecosystems has not stopped, and modern oceanography is attracting a renewed interest, mainly driven by the development of innovative technological solutions for the exploration and study of the ocean life, global climate change, and for the collection of scientific data.

Specific examples include unmanned vehicles for the exploration and monitoring of the seabed and marine environments, such as autonomous underwater vehicles (AUVs) and remotely operated vehicles (ROVs)[1,2]. The data collected by those vehicles are required to be transmitted through a reliable communication link, with data rates ranging from one to tens of megabits per second (Mbit/s).

However, the high costs and lack of flexibility of the wireline systems become restrictive for many of these applications[3]. Therefore, there is a considerable effort in the development of new solutions for underwater wireless communications (UWCs).

Despite the efforts made so far, the UWC still remains quite challenging, due to the unique and harsh conditions that characterize underwater channels. The main issues include severe attenuation, link distances, and limited resource utilization. Nonetheless, many academic and industrial researchers have paid attention to the development of state-of-the-art solutions exploiting acoustic and electromagnetic (EM) waves.

Nowadays, underwater acoustic wireless communications (UAWCs) are the most used UWC technology. First UAWC systems date back to the 19$^{\text{th}}$ century, and they were widely used during the World Wars for military purposes. They are still the most diffused technology, thanks to their long communication range (up to several kilometers)[4,5], which is very attractive considering the hugeness of the oceans. During the years, there have been many technological advances, although they are unable to overcome the key physical limitation of acoustic waves.

As is known, acoustic technology is limited in data rate. This is mainly determined by two different factors: the low bandwidth of the acoustic waves and the delay spread, which leads to severe inter-symbol interference (ISI). The nominal propagation speed of the acoustic waves, of around 1500 m/s, causes latency in the order of seconds, limiting the system for real-time and multimedia applications. The actual speed value strongly depends on water temperature, salinity, and depth. In addition, acoustic waves require high power, and it must be taken into account that any anthropogenic source of sound could impact detrimentally on marine animals[6]. Nevertheless, UAWC systems are commonly used to provide command and control applications.

Unlike acoustic waves, radio frequency (RF) signals can provide higher propagation and transmission speeds and are more tolerant to turbulence and turbidity effects of water. Also, there is an already available huge and strong knowledge on terrestrial RF communication, which may be exploited to realize the RF-UWC modems. However, RF waves suffer from serious attenuation in water, which increases with the frequency: e.g., more than 180 dB/m for the 2.4 GHz bandwidth[7–9].

A complete RF attenuation curve as a function of the frequency is reported in Fig. 1.

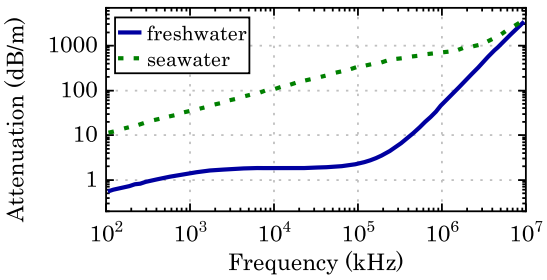

Fig. 1. Radio frequency attenuation in water[7–9].

The use of ultra-low frequencies could reduce the attenuation levels at the expense of high hardware costs, low data rates, and, above all, huge antennas (at 10 kHz, the wavelength is 30 km).

Considering the aforementioned constraints for acoustic and RF waves, optical waves have been recently proposed as an alternative solution. Optical waves, indeed, can provide high-speed transmission and low latencies, with the drawback of a limited communication range (ten to hundreds of meters). When targeting short-range UWC, it is possible to exploit the low-attenuation window in the EM spectrum, which lies in the visible region around the blue wavelength, as can be seen in Fig. 2.

In the last decade, the impressive developments of light emitting diodes (LEDs) for lighting purposes made widely available compact devices of low-cost and significant modulation bandwidth. Thus, underwater optical wireless communication (UOWC) gained popularity and various prototypes and commercial products are now available.

Table 1 presents a comparison between the three types of UWC systems, showing the differences in their main parameters.

The three technologies mentioned above have clearly different applications in the underwater environment, but, if we consider a complex scenario, they can be complementary. As an example, the UWC scenario presented in Fig. 3 consists of many distributed nodes, such as ships, AUVs, ROVs, seabed sensors, buoys, and scuba divers.

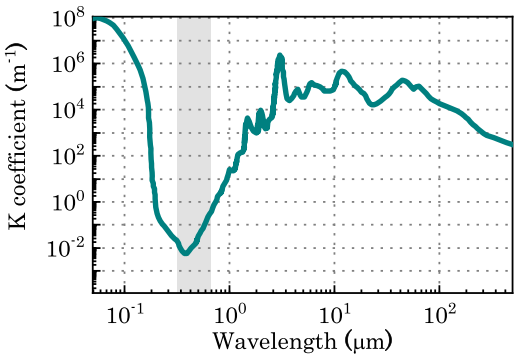

Fig. 2. Attenuation curve at different wavelengths[10].

Table 1. Comparison of the Three UWC Technologies

Parameter	Acoustic	RF Waves	Optical Waves
Link range	<25 km	<10 km	1–100 m
Data rate	<12 kbit/s	Few Mbit/s	1–1000 Mbit/s
Attenuation	0.1–4 dB/km	10–180 dB/m	0.4–11 dB/m
Latency	High	Low	Low
Cost	High	High	Low
Size	High	High	Low

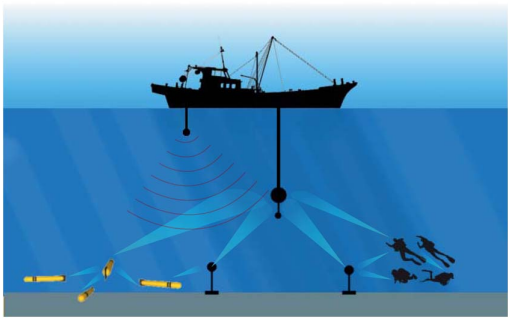

Fig. 3. Underwater wireless communication scenario.

All of the mobile nodes communicate with the others wireless, sharing data and collaborating for the monitoring of the underwater environment. Then, AUVs and ROVs convey the signals to buoys, which are wired to be connected with ships above the sea surface. High-speed data transmissions are based on UOWC systems, whilst command and control links are realized with UAWC technology. In this way, hybrid acoustic/optical UWC exploits the advantages of each communication technology to increase the reliability of the underwater network.

Here, we provide a comprehensive survey on the UOWC technologies, showing the pros and cons of the different implementations. There are several issues that must be taken into account when designing a UOWC modem. In the following, we report the main challenges to be considered: attenuation and background light. Because of the peculiar channel, it is useful to understand some basic optical properties of light propagation in water. Absorption and scattering are the two main inherent phenomena that contribute to the optical signal attenuation in water. Absorption is due to both inorganic and organic substances that convert the photon's energy into other forms, such as heat and chemical (photosynthesis), reducing the optical beam intensity. Scattering is a deflection of the photons from the original direction, caused by the interaction with the molecules and the atoms within water, which widens the range of incident angles on the receiver (RX). Both of these effects limit the overall transmission distance. Moreover, the scattering also causes a spread in the photon's time arrival, and this may lead into multipath interference and ISI in high-speed UOWC links (>1 Gbit/s)[11]. The overall underwater losses are, thus, usually expressed by the attenuation coefficient $k(\lambda)$, which is given by

$$k(\lambda) = a(\lambda) + b(\lambda), \tag{1}$$

where $a(\lambda)$ and $b(\lambda)$ are the absorption and scattering coefficients, respectively. These coefficients strongly depend on specific water conditions and on the wavelength of the optical source. In pure sea water, the minimum in the attenuation curve is at 470 nm. This minimum shows a red-shift in murkier water. Experimental curves are reported in Fig. 4[10].

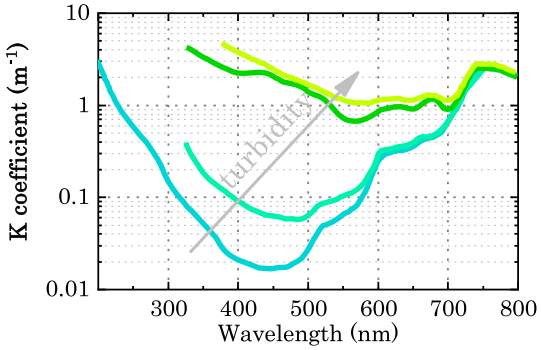

Fig. 4. Attenuation curve in the visible region, at increasing water turbidity[10].

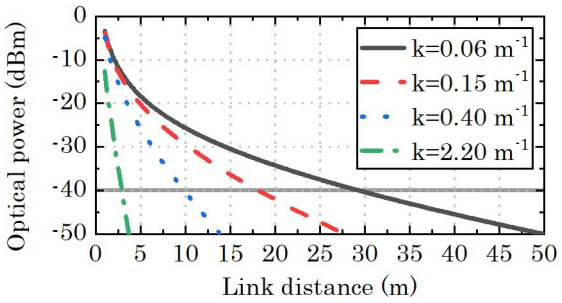

Fig. 5. Simulated received optical power as a function of the link distance at different values of water turbidity. Straight gray line indicates the receiver sensitivity.

Table 2. Typical Absorption and Scattering Coefficients[12]

Water Types	$a(\lambda)$	$b(\lambda)$	$k(\lambda)$
Pure sea	0.05	0.01	0.06
Clear ocean	0.11	0.04	0.15
Coastal ocean	0.2	0.2	0.4
Turbid harbor	0.3	1.9	2.2

Usually, the water types are classified as pure sea, clear ocean, coastal ocean, and turbid harbor water; the corresponding typical k values are summarized in Table 2.

In pure water, the light beam propagates in a straight line with very low dispersion, and the absorption is the main limiting factor. At the opposite, in turbid harbor water, the scattering effect becomes dominant, widening the light beam.

The most widely used model to describe the UOWC channel attenuation is the Beer–Lambert (BL) Law. This model allows us to estimate the power losses due to absorption and scattering after propagation in a water channel. The BL expression is given by

$$P(d,\lambda) = P_0 e^{-k(\lambda)d}, \tag{2}$$

where P_0 is the reference optical power, and d is the link distance. Considering a directed line-of-sight (DLOS) configuration, the BL Law assumes that all the scattered photons are lost, since it ignores the multi-path arrival of the scattered photons. Thus, the estimation of P may be lower compared to the actual one, especially for long transmission links.

The knowledge of these mechanisms is very useful in estimating the transmission distance. A simulation of a link budget for different turbidity values is presented in Fig. 5 as an example. The curves are obtained exploiting the BL model and the proportionality to d^{-2}, typical of free-space links[13]:

$$P_{\mathrm{RX}} = P_{\mathrm{TX}}\left[\frac{A e^{-k(\lambda)d}}{\pi d^2}\right], \tag{3}$$

where P_{TX} and P_{RX} are the transmitted and received optical power, respectively, and A is the area of the RX. In this example, we considered an LED array emitting 5 W optical power with 120° emission angle, a photo-diode (PD) active area of 1 cm^2, and an RX sensitivity of −40 dBm.

As can be seen, in clear sea water ($k = 0.06$ m^{-1}), a link of 30 m can be achieved, whilst in turbid harbor water ($k = 2.2$ m^{-1}) only 2–3 m can be reached. It is worth noting that these curves are given as an example; further distances can be reached, introducing, e.g., optical elements in front of the transmitter (TX) and the RX.

A more exhaustive channel modeling is the two-term Henyey–Greenstein (TTHG), which includes an analytic function to describe the photon's phase distribution due to scattering effects[14–16]. The TTHG model was originally proposed for galactic astrophysics[17] and then readapted for the underwater environment. However, experimental studies show that the difference between the two models is limited only to short distances (or low-turbidity water) and is notable only for large product values of attenuation coefficient and distance ($k \cdot d > 10$)[18].

In practical cases (especially in shallow waters), the background light may reach high values (up to ∼10^5 lx on direct sunlight). The intensity, obviously, depends on the working depth: e.g., in deep ocean, it is by far lower than in shallow harbor waters. In order to have the UOWC capable of working in all conditions, the impairments of the sunlight cannot be neglected and must be considered when designing the optical system. Clearly, the sunlight can be strongly attenuated exploiting a band-pass filter to reject the ambient light outside of the emission window $\Delta\lambda$ of the optical source. The background light received by the photo-detector P_{BG} can be factorized with several parameters and is given by

$$P_{\mathrm{BG}} = A(\pi\theta)^2 f(\lambda) L_{\mathrm{SUN}}(\Delta\lambda), \tag{4}$$

where θ is the field-of-view (FOV) of the RX, $f(\lambda)$ is the optical band-pass filter transmittivity, and L_{SUN} is the solar radiance integrated in the $\Delta\lambda$ wavelength region. All these parameters must be considered in order to minimize the effect of the background light. The main

effect of a strong ambient light is the saturation that occurs on the photo-detector: the higher the received background optical power is, the lower the AC photocurrent generated is, heavily reducing the RX sensitivity. Clearly, different types of photo-detectors may show different behaviors.

The performance of a UOWC system can also be affected by channel fading as a result of ocean turbulence. Indeed, variations in the refractive index caused by turbulent water can slightly and continuously change the propagation direction of photons. Those refractive index changes are mainly due to temperature, salinity, and pressure variations in water[19]. Since these effects are more present in shallow waters, most of the works used to neglect them.

Two light sources are commonly used in UOWC systems: LED and laser diode (LD). A comparison of parameters between these two electro-optical devices is reported in Table 3.

LEDs have the advantages of being cheap, high power, and reliable devices, with a low-temperature dependence, but they show a wide spectral bandwidth, therefore requiring wide band-pass filters, which, in turn, cause solar background noise to enter in the system. LDs have a short switching time and a very narrow optical emission, but they may require a proper cooling system. Depending on the specific application, the two solutions are alternative: for really high-speed UOWC links (≥1 Gbit/s), LDs would be the preferable choice thanks to the wider electrical modulation bandwidth; on the other hand, if a robust communication with a moderate speed (1–100 Mbit/s) is required, LEDs would be the right choice.

Regarding the RX, the most common photo-sensors in the visible region are the photo-multiplier tubes (PMTs) and the PDs, which include both positive-intrinsic-negative (PIN) and avalanche PDs (APDs). A PMT is a long vacuum tube, with an electronic sensor extremely sensitive to visible light. It has low noise, high gain, and wide active area at the expense of being bulky, energy hungry, and expensive. Few experimental demonstrations exploit PMTs in UOWC[20–23]. A PIN-PD is characterized by fast response, low cost, unity gain, and good tolerance to ambient light, whereas an APD has large internal gain, high quantum efficiency (>70%), and better sensitivity, but requires high bias voltage, complex control circuitry, and is more sensitive to ambient light. Experimental demonstrations were realized with both PD devices[24–28].

Table 3. Comparison Between Optical Sources for UOWC

Parameter	LED	LD
Optical power	1 W	10–1000 mW
Optical bandwidth	20–50 nm	1–2 nm
Electrical bandwidth	10–15 MHz	0.6–1 GHz
Beam emission angle	120°	20°
Thermal management	Mildly needed	Strongly needed
Cost	Low	High

Recently, many theoretical and experimental works on UOWC have been presented. Few UOWC modems were also commercialized in the past: Ambalux introduced a commercial UOWC system, claimed to transmit 10 Mbit/s over 40 m. Also, Sonardyne made available a product in two versions: one claimed to transmit 5 Mbit/s in 10 m range in "high ambient light conditions" and the other 12.5 Mbit/s in ranges up to 150 m, "suitable for moderate to low-turbidity dark water"[29]. However, very limited information is available about these systems.

In Table 4, we report a list of the noticeable experimental academic results (from 2015), with either LDs or LEDs as an optical source and a PIN-PD or APD as an optical RX. In these works, different bit rates were targeted, from a few Mbit/s to several gigabits per second (Gbit/s), reaching various transmission distances. All of them are implemented in DLOS, rather than the diffuse configuration like in acoustic and RF wave systems. This architecture allows it to be more energy efficient and effective against eavesdroppers.

Gigabit rates were demonstrated exploiting LDs and advanced modulation format such as orthogonal frequency division multiplexing (OFDM) or pulse-amplitude modulation (PAM) at a distance of several meters. A record speed of 30 Gbit/s was achieved with a complex setup based on beam reducer–expander and the two-stage injection locking technique[30]. In Ref. [28], the authors exploit a blue LED and a pre-equalized OFDM signal to achieve 3 Gbit/s transmission over a 1.2 m water channel. These achievements were all quite impressive; nevertheless, most of them were proved in a very controlled environment, where the underwater channel was simulated using a water tank. In many cases TX and RX were out of water. This solution, although correct for preliminary measurements, has very limited challenges: water turbidity (usually tap water), background light (laboratory common illumination), and small turbulences are not actually addressed. Indeed, in an optical system that requires perfectly aligned links, turbulence may cause a complete signal loss.

In Fig. 6, we report some typical experimental setups for underwater demonstrations in laboratory environments, with water tanks used to simulate underwater scenarios.

In order to emulate the different refractive conditions and turbidity typical of underwater environments, Maalox is usually added to the water as a scattering agent for attenuating the light beam[31–33].

Only a few works performed transmission tests in a real sea environment[23,35,36]. In Refs. [23,37], the authors presented a UOWC system, tested in the Juan de Fuca plate at a depth of 2400 m. The optical modem was developed by the Optical Communication Group at Woods Hole Oceanographic Institution (WHOI). They

demonstrated an LED-based bi-directional transmission over long ranges (>100 m in clear, dark water) without the need to align the TX and RX.

Figure 7 shows the optical modem and the experimental setup used during the sea test. However, the authors do not provide the complete characterization of the UOWC system, and no indication on the devices is reported.

Another UOWC demonstration, tested in harbor water of Rhode Island (USA), is reported in Refs. [36,38]. The authors presented a real-time uni-directional transmission at 4.8 m, with a measured attenuation coefficient slightly higher than 1 m^{-1} (high-turbidity water). The TX consisted of a laser emitting at 515 nm, collimating optics, and a steering mirror. The RX included another steering mirror, a focal plane camera (for alignment purposes), and an APD (see Fig. 8). The communication rate was 125 Mbit/s, exploiting the on–off keying non-return-to-zero (OOK-NRZ) modulation format. The tests were conducted through a variety of conditions over five days, including day and night.

In Refs. [35,39], the authors presented a novel pair of optical wireless modems, which exploit blue LEDs to transmit 10Base-T Ethernet standard signals through water. The modems were tested in shallow water in Italy (La Spezia Harbor), transmitting bi-directionally 10 Mbit/s over up to 10 m despite the high turbidity [≥3 formazin turbidity unit (FTU)] and the strong sunlight (−21 dBm, 10 dB more than optical signal power).

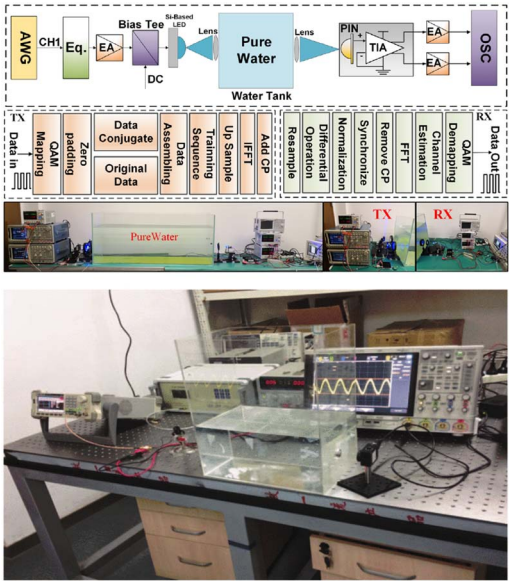

Fig. 6. Examples of two experimental setups for underwater demonstrations in the laboratory environment[28,34].

The optical modem is represented in Fig. 9, which shows a schematic of the electro-optical devices, the pictures of one modem, and of the experimental setup for the field sea trial. The system was tested at different distances, different water turbidity types, and different ambient light conditions for a complete characterization. One of

Table 4. Noticeable Experimental Results for UOWC Systems from 2015

Year	Bit Rate (Mbit/s)	Distance (m)	Water	Optical Source	λ (nm)	Test	Modulation Format	Ref.
2015	10	70	Clean	LED	N.A.	Ocean	OOK-NRZ	[23]
2015	20	0.3	Clean	Laser	Red	Water tank	OOK-NRZ	[34]
2015	1450	4.8	Clean	LD	405	Water tank	OFDM	[40]
2015	2300	7	Clean	LD	520	Water tank	OOK-NRZ	[41]
2015	4800	5.4	Clean	LD	450	Water tank	OFDM	[27]
2016	1500	20	Clean	LD	450	Water tank	OOK-NRZ	[42]
2016	200	5.4	Clean	μLED	440	Water tank	OOK-NRZ	[43]
2016	125	4.8	Turbid	Laser	515	Harbor	OOK-NRZ	[36]
2017	3	N.A.	N.A.	LED	N.A.	Water tank	N.A.	[44]
2018	2700	34.5	Clean	LD	520	Water tank	OOK-NRZ	[45]
2018	10	10	Turbid	LED	470	Harbor	Manchester	[35]
2018	9700	2.3	Clean	LD	RGB	Water tank	OOK-NRZ	[46]
2019	30,000	12.5	Clean	LD	487	Water tank	PAM4	[30]
2019	3000	1.2	Clean	LED	Blue	Water tank	OFDM	[28]
2019	500	100	Clean	LD	520	Water tank	OOK-NRZ	[47]
2019	30	14.7	Clean	LD	450	Water tank	OOK-NRZ	[48]
2019	50	3	Clean	LD	450	Water tank	16-QAM	[49]

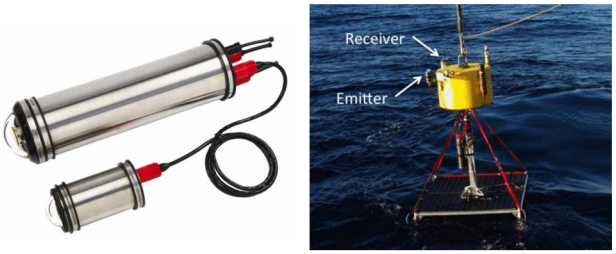

Fig. 7. (a) Picture of the WHOI optical modem; (b) test node with an optical modem installed on top[23].

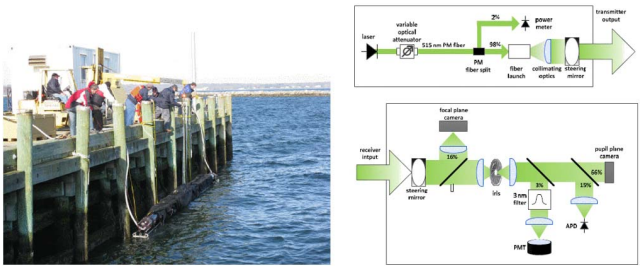

Fig. 8. Experimental setup of the sea-trial measurements (left); scheme of the UOWC modem (right)[36].

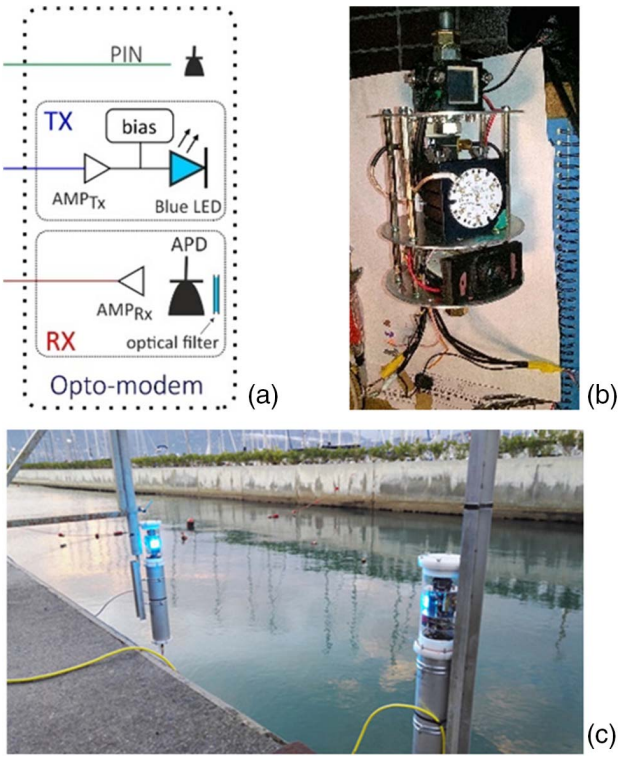

Fig. 9. (a) Scheme of the UOWC modem and (b) picture of one of them. The three layers contain a monitor PD, the LEDs, and the receiver[34]. (c) Experimental setup of the sea-trial measurements.

the modems was also tested on top of an ROV to verify the robustness of the link to misalignment. The communication was successfully completed within a range of 5 m.

The communication systems for ocean exploration require a clear understanding of the propagation mechanisms related to different underwater signals.

In this survey, we provided an overview on UWCs, focusing on the state of the art of the recent achievements that exploit the optical technology. Table 1 summarizes the main pros and cons of each presented UWC technology, defining the clear advantages of acoustic and optical waves compared to the RF solution for underwater communication networks. RF signals for UWC can be used only at extremely low frequencies because of the heavy absorption at higher frequencies, failing to reach a high-speed alternative to acoustic waves. UOWC provides great potential to overcome the UAWC drawbacks, thanks to the higher data rate, lower latency, and power consumption solution at the expense of a reduction of the link distance.

We strongly believe that, if the ongoing research and the future technology implementation of UOWCs will assist the process, the hybrid acoustic/optical modem is the viable solution for a robust and feasible underwater communication network.

The author thanks E. Ciaramella, A. Caiti, A. Sturniolo, A. Messa, and S. Greco for the useful comments and discussions.

References

1. K. Alam, T. Ray, and S. G. Anavatti, Ocean Eng. **88**, 627 (2014).
2. M. Kojima, A. Asada, K. Mizuno, K. Nagahashi, F. Katase, Y. Saito, and T. Ura, in *Proceedings of Autonomous Underwater Vehicles 2016* (2016), paper AUV161.
3. S. D. Ling, I. Mahon, M. P. Marzloff, O. Pizarro, C. R. Johnson, and S. B. Williams, Limnol. Oceanogr. Methods **14**, 293 (2016).
4. T. Melodia, H. Kulhandjian, L.-C. Kuo, E. Demirors, S. Basagni, M. Conti, S. Giordano, and I. Stojmenovic, *Mobile Ad Hoc Networking: Cutting Edge Directions* (Wiley, 2013), p. 804.
5. J. Kassem, E. Kranakis, and S. Porretta, in *Proceedings of 9th International Conference on Ad Hoc Networks* (2018), p. 3.
6. M. Solan, C. Hauton, J. A. Godbold, C. L. Wood, T. G. Leighton, and P. White, Sci. Rep. **6**, 20540 (2016).
7. L. B. VK5BR, Amateur Radio (1987).
8. M. Lanzagorta, *Underwater Communications* (Morgan and Claypool, 2012).
9. F. Teixeira, J. Santos, L. Pessoa, M. Pereira, R. Campos, and M. Ricardo, in *Proceedings of 10th ACM International Conference on Underwater Networks and Systems* (2015), paper WUWNet 2015.
10. N. G. Jerlov, *Marine Optics* (Elsevier Scientific, 1976).
11. A. S. Fletcher, S. A. Hamilton, and J. D. Moores, IEEE Commun. Mag. **53**, 49 (2015).
12. J. W. Giles and I. N. Bankman, in *IEEE Military Communications Conference* (2005), p. 1.
13. J. M. Kahn and J. R. Barry, Proc. IEEE **85**, 265 (1997).
14. H. C. Hulst and H. C. van de Hulst, *Light Scattering by Small Particles* (Courier, 1981).
15. C. D. Mobley, *Light and Water: Radiative Transfer in Natural Waters* (Academic, 1994).
16. V. I. Haltrin, Appl. Opt. **41**, 1022 (2002).
17. L. G. Henyey and J. L. Greenstein, Astrophys. J. **93**, 70 (1941).
18. B. Cochenour, L. Mullen, and J. Muth, Opt. Lett. **35**, 2088 (2010).

19. J. A. Simpson, B. L. Hughes, and J. F. Muth, in *Proceedings of OCEANS 2009* (2009), p. 1.
20. M. Khalighi, T. Hamza, S. Bourennane, P. Léon, and J. Opderbecke, IEEE Photon. J. **9**, 7905310 (2017).
21. J. A. Simpson, "A 1 Mbps Underwater Communications System using LEDs and Photodiodes with Signal Processing Capability," Master thesis (North Carolina State University, 2008).
22. M. Sun, B. Zheng, L. Zhao, X. Zhao, and F. Kong, in *Proceedings of OCEANS 2014* (2014), p. 1.
23. C. Pontbriand, N. Farr, J. Hansen, J. C. Kinsey, L.-P. Pelletier, J. Ware, and D. Fourie, in *Proceedings of OCEANS 2015* (2015), p. 1.
24. M. Doniec, I. Vasilescu, M. Chitre, C. Detweiler, M. Hoffmann-Kuhnt, and D. Rus, in *Proceedings of OCEANS 2009* (2009), p. 1.
25. F. Hanson and S. Radic, Appl. Opt. **47**, 277 (2008).
26. M. Doniec, C. Detweiler, I. Vasilescu, and D. Rus, in *Proceedings of 2010 IEEE/RSJ International Conference on Intelligent Robots and Systems* (2010), p. 4017.
27. H. M. Oubei, J. R. Duran, B. Janjua, H.-Y. Wang, C.-T. Tsai, Y.-C. Chi, T. K. Ng, H.-C. Kuo, J.-H. He, and M.-S. Alouini, Opt. Express **23**, 23302 (2015).
28. F. Wang, Y. Liu, M. Shi, H. Chen, and N. Chi, Opt. Eng. **58**, 056117 (2019).
29. Sonardyne, https://www.sonardyne.com/product/bluecomm-underwater-optical-communication-system.
30. W.-S. Tsai, H.-H. Lu, H.-W. Wu, C.-W. Su, and Y.-C. Huang, Sci. Rep. **9**, 8605 (2019).
31. W. C. Cox, K. F. Gray, J. A. Simpson, B. Cochenour, B. L. Hughes, and J. F. Muth, in *Proceedings of OCEANS 2010* (2010), p. 1.
32. S. A. Adnan, M. A. Ali, A. C. Kadhim, M. Sadeq, and M. Riaz, in *Proceedings of Light, Energy and the Environment* (2017), paper JW5A.14.
33. A. Keskin, F. Genç, S. A. Arpali, Ö. K. Çatmakaş, Y. Baykal, and Ç. Arpali, in *Proceedings of 2015 4th International Workshop on Optical Wireless Communications (IWOW)* (2015), p. 41.
34. A. Lin, W. Lu, J. Xu, H. Song, F. Qu, J. Han, X. Gu, and J. Leng, in *Proceedings of OCEANS 2015* (2015), p. 1.
35. G. Cossu, A. Sturniolo, A. Messa, S. Grechi, D. Costa, A. Bartolini, D. Scaradozzi, A. Caiti, and E. Ciaramella, J. Light. Technol. **36**, 5371 (2018).
36. A. S. Fletcher, C. E. Devoe, I. D. Gaschits, F. Hakimi, N. D. Hardy, J. G. Ingwersen, R. D. Kaminsky, H. G. Rao, M. S. Scheinbart, T. M. Yarnall, and S. A. Hamilton, in *Proceedings of OCEANS 2016* (2016), p. 1.
37. N. E. Farr, J. D. Ware, C. T. Pontbriand, and M. A. Tivey, in *Proceedings of OCEANS 2013* (2013), p. 1.
38. H. G. Rao, C. E. Devoe, A. S. Fletcher, I. D. Gaschits, F. Hakimi, S. A. Hamilton, N. D. Hardy, J. G. Ingwersen, R. D. Kaminsky, M. S. Scheinbart, and T. M. Yarnall, in *Proceedings of OCEANS 2016* (2016), p. 1.
39. G. Cossu, A. Sturniolo, A. Messa, D. Scaradozzi, and E. Ciaramella, IEEE J. Sel. Areas Commun. **36**, 194 (2018).
40. K. Nakamura, I. Mizukoshi, and M. Hanawa, Opt. Express **23**, 1558 (2015).
41. H. M. Oubei, C. Li, K.-H. Park, T. K. Ng, M.-S. Alouini, and B. S. Ooi, Opt. Express **23**, 20743 (2015).
42. C. Shen, Y. Guo, H. M. Oubei, T. K. Ng, G. Liu, K.-H. Park, K.-T. Ho, M.-S. Alouini, and B. S. Ooi, Opt. Express **24**, 25502 (2016).
43. P. Tian, X. Liu, S. Yi, Y. Huang, S. Zhang, X. Zhou, L. Hu, L. Zheng, and R. Liu, Opt. Express **25**, 1193 (2017).
44. Z. Song, E. Schwartz, and K. Mohseni, in *Proceedings of 2017 IEEE SENSORS* (2017), p. 1.
45. X. Liu, S. Yi, R. Liu, L. Zheng, and P. Tian, Opt. Express **25**, 27937 (2018).
46. X. Liu, S. Yi, X. Zhou, S. Zhang, Z. Fang, Z.-J. Qiu, L. Hu, C. Cong, L. Zheng, R. Liu, and P. Tian, Opt. Express **26**, 19259 (2018).
47. J. Wang, C. Lu, S. Li, and Z. Xu, Opt. Express **27**, 12171 (2019).
48. Y. Han, Y. Zheng, K. Shi, T. Wang, X. Xie, J. Meng, W. Wang, T. Duan, B. Han, R. Wan, and K. Sun, Proc. SPIE **11068**, 110680U (2019).
49. J. Wang, C. Tian, X. Yang, W. Shi, Q. Niu, and T. A. Gulliver, Appl. Opt. **58**, 4553 (2019).